Sciences & Technologie A – N°46, Décembre 2017, 35-44

STRUCTURAL AND ELECTRONIC PROPERTIES OF AL1-XINXN IN WURTZITE AND ZINCBLENDE PHASES: A COMPARATIVE TIGHT BINDING AND DFT STUDY.

Abdelhakim Meziani[1,2], Lemia Semra[2], Tarik Ouahrani[3], Azzedine Telia[2], Hilmi Ünlü[4]

1 Physics Department Frères Mentouri University Constantine, 25000 Algeria.
2 Laboratory of Microelectronics and instrumentation, Electronics department, Frères Mentouri University Constantine, 25000 Algeria.
3 Laboratoire de Physique Théorique, Université de Tlemcen, BP 230, 13000 Tlemcen, Algeria.
4 İstanbul Technical University, Faculty of Science and Letters, Department of Physics Engineering, Maslak, 34469 İstanbul, Turkey.

Reçu le 03/01/2017 – Accepté le 12/11/2017

Abstract

We present a comparative theoretical study on the structural and electronic properties of $Al_{1-x}In_xN$alloy in both zincblende and wurtzite phases based on the semiempirical sp^3s^* tight binding model with nearest neighbor interactions and density functional theory with modified Becke–Johnson potential (mBJLDA). Optimizing the lattice parameters, the physical parameters such as band gap, effective mass, density of states and charge density were calculated for the entire composition range of $Al_{1-x}In_xN$alloy. Results of the calculations made by both theories are found to be in good agreement for both zincblende and wurtzite phases.

Keywords: *AlInN alloy, nearest neighbor sp3s*tight binding model, DFT with modified Becke–Johnson potential (mBJLDA).*

Résumé

Nous présentons une étude théorique comparative sur les propriétés structurales et électroniques de Al1-xInxNalloy dans les phases de zincblende et de wurtzite basées sur le modèle de liaison étroite semi-empirique sp^3s * avec interactions de plus proches voisins et théorie fonctionnelle de la densité avec potentiel de Becke-Johnson modifié (mBJLDA). En optimisant les paramètres de réseau, les paramètres physiques tels que la bande interdite, la masse effective, la densité d'états et la densité de charge ont été calculés pour toute la plage de composition de $Al_{1-x}In_xN$alloy. Les résultats des calculs effectués par les deux théories sont en bon accord pour les phases de zincblende et de wurtzite.

Mots clés *: Alliage AlInN, modèle le plus proche du sp3s * le plus proche, DFT avec le potentiel de Becke – Johnson modifié (mBJLDA).*

ملخص

نقدم دراسة نظرية مقارنة حول الخصائص البنيوية والإلكترونية لـ Al1 – xInxNalloy في كلا مرحلتين zincblende و wurtzite على أساس semiempirical sp3s * نموذج الربط الضيق مع أقرب تفاعلات الجوار والنظرية الوظيفية للكثافة مع إمكانات Becke – Johnson المعدلة (mBJLDA). تم حساب الحد الأمثل لمعلمات الشبكة ، المعلمات المادية مثل فجوة النطاق ، الكتلة الفعالة ، كثافة الولايات وكثافة الشحنة لنطاق التركيب الكامل لـ Al1 – xInxNalloy. تم العثور على نتائج الحسابات التي أجريت من قبل كل من النظريات لتكون في اتفاق جيد لكل من مراحل zincblende و wurtzite.

الكلمات المفتاحية : سبيكة AlInN ، أقرب جارات sp3s * نموذج ملزم ضيق ، DFT مع إمكانات Becke – Johnson المعدلة (mBJLDA).

INTRODUCTION

The semiconductor ternary alloy $Al_{1-x}In_xN$ has a band gap that covers a very wide energy range (0.69 eV to 6.25 eV) [1], which makes it an ideal candidate for a range of electronic and optoelectronic devices such as high electron mobility transistors (HEMTs) for high-frequency and high-power microwave applications [2] and also for the application in highly-reflecting distributed Bragg reflectors (DBRs), light-emitting diodes (LEDs), laser diodes (LDs), detectors and sensors [3]. Both AlN and InN crystallize in wurtzite structure. However, the stabilization in zincblende structure of these compounds by molecular beam epitaxy has also been achieved [4]. Subsequently, it is well known that the ternary $Al_{1-x}In_xN$alloy can occur in both forms.

In this work we present a theoretical study of the structural and electronic properties of $Al_{1-x}In_xN$ in these two phases. This study is carried by first principles using DFT and by semi-empirical tight binding method (TB).In order to improve the DFT band gap calculations we used the potential introduced by Tran Blaha [5],which gives a good correction to the gap, and the optimized values calculated from DFT will be associated with the tight binding calculation for ternary compounds. We will investigate the variation with alloy composition x of various physical entities such as the energy band gap, the electron effective mass, the density of states and charge density and will compare with available experimental/first principle data. We will also derive and compare related bowing parameters of these two zincblende and wurtzite phases.

2. COMPUTATIONAL DETAILS

2.1 Density Functional Theory Calculation

We have performed DFT-based ab-initio calculations within the full potential linearized augmented plane wave (FP-LAPW) method as implemented in Wien2k code [6]. In the FP-LAPW method, the unit cell volume is partitioned in two regions, muffin tin spheres (around each nucleus) and interstitial region. Inside each atomic sphere the wave function is approximated by a linear combination of radial functions times spherical harmonics, while in the interstitial region a plane wave expansion is used, with an energy separation between valence and core states of 6 Ry. For the total energy calculations, we utilize the Perdew, Burke and Ernezerhof (PBE) [7] functional for exchange and correlation in LDA. Since PBE underestimates band gaps the mBJLDA [5] a modified version of the Becke-Johnson potential was employed for the electronic calculations to improve band gaps. We used a sampling grid of about 1500 k-points in the irreducible Brillouin zone (IBZ) for both binary compounds structures. The convergence of the basis set is controlled by a cutoff parameter $R_{mt}K_{max}$= 7 and l_{max}=10 to ensure a convergence of total energy to an accuracy of 0.1 mRy. Starting from bulk AlN structure we obtained the ternary $Al_{1-x}In_xN$(x=0.25, 0.5, 0.75, 1) by replacing the Al atoms with In in the supercell. For the wurtzite structure of the ternary we carried out calculation with a supercell of 16 atoms (2x2x1) using an ordered form, whereas for the zincblende form a supercell having luzonite structure for x=0.25, 0.75 and a chalcopyrite for x=0.50 was used.

2.2 Semi-empirical tight binding model

We have adopted the nearest neighbor (NN)*sp3s** tight binding model which should prove sufficiently precise regarding electronic properties. In this model every atom is described by valence s orbital and the outer p orbital and an *s** state to reproduce high orbital states [8]. The spin orbit effect is neglected regarding the type of atoms used. The tight binding parameters on-site energies E_{sa}, E_{sc}, E_{pa}, E_{pc}, E_{s^*a}, E_{s^*c} and the off diagonal elements V_{ss}, V_{xx}, V_{sapc}, V_{scpa}, V_{xy}, V_{s^*p}, $V_{p^*s}$are obtained from experimental data for band gap energies [9] and modified so as to reproduce energies at high symmetry points. The Schrodinger equation in matrix form is:

$$\sum_{\beta}[H_{\alpha\beta}(k)-S_{\alpha\beta}(k)E]u_{\beta}=0, \quad (1)$$

where E is the energy eigenvalue of the 10x10 Hamiltonian matrix:

$$H_{\alpha\beta}(k)=<\chi_{\alpha}(k)\,|\,H\,|\,\chi_{\beta}(k)>, \quad (2)$$

with the overlap integral between the atomic-like orbitals, with α and β that correspond to cation (c) and anion (a) s, p atomic orbitals, respectively.

$$S_{\alpha\beta}(k)=<\chi_{\alpha}(k)\,|\,\chi_{\beta}(k)>, \quad (3)$$

χ(k) is the basis function formed by the linear combination of cation and anion s, p atomic orbitals. Using the derived parameters, the energy bands are obtained by diagonalizing the Hamiltonian matrix at each point of the Brillouin zone.

The calculation of atomic energies for the $Al_{1-x}In_xN$ ternary is carried out by using the virtual crystal approximation

$$E_{vi}(x)=xE_{vi,AlN}+(1-x)E_{vi,InN}, \quad (4)$$

$$V_{vi}(x)=xV_{vi,AlN}+(1-x)V_{vi,InN}, \quad (5)$$

where $i=s, p_x, p_y, p_z, s^*$ and $v=\alpha, \beta$ *with* $V_{vi}= V_{ss}, V_{xx}, V_{sapc}, V_{scpa}, V_{xy}, V_{s^*p}, V_{p^*s}$.

2.3 Charge Density Calculation

The electron localization function (ELF), first introduced by Becke and Edgecombe[10], provides a measure of the localization of electron pairs in atomic and molecular systems which are able to recover the chemical representation of a molecule consistent with Lewis valence picture. The ELF has been defined as to have values between 0 and 1 (1 corresponding to perfect localization) in order to ease the visualization of its surfaces. The topological analysis of ELF surfaces provides a partition of the three-dimensional space into non-overlapping basins which can be thought of as electronic basins corresponding to bonds (B), lone pairs (LP),and atomic core shells (C). Hence, the integration of the density over their volumes assigns a population to the basins.
These populations are well known [11] to follow the expected values and tendencies from the Aufbau principle and the valence shell electronic pair repulsion (VSEPR) theory. All electron wave functions are preferable for a quantitative analysis of the ELF topology in a crystalline phase.

3. Results and Discussion

3.1 Structural properties

The equilibrium structural parameters were determined by fitting the total energy versus volume to Murnaghan's equation of states [12]:

$$E(V) = E_0 + \frac{B_0 V}{B_0^{'}}\left(\frac{(V_0/V)^{B_0}}{B_0^{'}-1}+1\right) - \frac{B_0 V}{B_0^{'}-1}, \quad \textbf{(6)}$$

where E_0 is the equilibrium energy, B_0 is the bulk modulus and B'_0 is its first derivative. Optimized values of the lattice parameter a of AlN and InN zincblende binaries are summarized in **Table 1**.

Table 1. Optimized lattice parameter for AlN and InN binaries with zincblende structure, compared with experiment and other theoretical works.

a_{Zb} (Å)	Optimized value	Other works	Experiment
AlN	4.383	4.396[a], 4.35[b], (4.353, 4.417)[c], 5.05[d], 4.995[e], 4.42[f], 4.308[g]	4.37[i], 4.38[j]
InN	4.991	4.947[b], 4.98[g], 4.96[h]	4.98[k], 4.986[l]

a: Ref. [20], b: Ref. [21],c: Ref. [22],d: Ref. [23],e: Ref. [24],f: Ref. [25],g: Ref. [17],h: Ref. [26],i: Ref. [13,27],j: Ref. [15,28],k: Ref. [13,15,27,29],l: Ref. [30].

The values obtained for AlN ($a_{op.}$= 4.383 Å) and for InN ($a_{op.}$= 4.991 Å) are comparable to the experimental ones (a_{AlN} = 4.38 Å and a_{InN} = 4.98 Å) [13].Similarly, the lattice parameters for wurtzite phase have been obtained by first optimizing u parameter then applying a 2D optimization. The results of optimized lattice parameters a and c are summarized in **Table 2**.

Table 2. Optimized lattice parameter for AlN and InN binaries with wurtzite structure, compared with experiment and other theoretical works.

Wz	Optimized value	Other works	Experiment
AlN			
a (Å)	3.113	3.124[a], (3.096, 3.139)[b], 3.1411[c], (3.092,3.127, 3.102)[d], 3.06[e], 3.125[f], 3.1437[g], 3.1411[h], 3.12225[i]	3.112 [j+k], 3.111[g] 3.11[l]
c (Å)	4.992	5.006[a], (4.959, 5.028)[b], 5.0268[c], (4.950,5.021,4.971)[d], 4.90[e], 5.008[f], 5.0311[g], 5.0268[h], 5.0518[i]	4.982 [j+k], 4.978[g], 4.98[l]
u	0.381	0.3805[h]	
InN			
a (Å)	3.538	3.58[m], 3.5440[c], (3.504,3.573, 3.548)[d], 3.572[e], 3.5920[g+i], 3.5440[h], 3.584[l]	3.548[n], 3.545[j], 3.540[d], 3.533[g]
c (Å)	5.72	5.78[o], 5.7228[p], (5.670, 5.762, 5.751)[c], 5775[q], 5.7879[r], 5.7228[s], 5.8119[t], 5.794[u]	5.760[l], 5.706[d], 5.693[g]
u	0.3785	0.380[v]	

a: Ref. [20], b: Ref. [22], c: Ref. [24], d: Ref. [31], e: Ref. [32], f: Ref. [33], g: Ref. [34], h: Ref. [35], i: Ref. [36], j: Ref. [15], k: Ref. [31], l: Ref. [37], m: Ref. [23], n: Ref. [14], o: Ref. [16], p: Ref. [17], q: Ref. [25], r: Ref. [27], s: Ref. [28], t: Ref. [29], u: Ref.[30], v: Ref.[13] .

$a_{op.}$= 3.113 Å and $c_{op.}$ = 4.992 Å for AlN binary and $a_{op.}$= 3.538 Å and $c_{op.}$ = 5.720 Å for InN binary. These values are similar to those obtained experimentally (a_{AlN} = 3.11 Å c_{aln} = 4.98 Å) and (a_{InN} = 3.540 Å and c_{inn} = 5.706 Å) [13]).The variation of optimized lattice parameters versus indium composition for both phases of $Al_{1-x}In_xN$ ternary alloy is illustrated in **Fig. 1**.

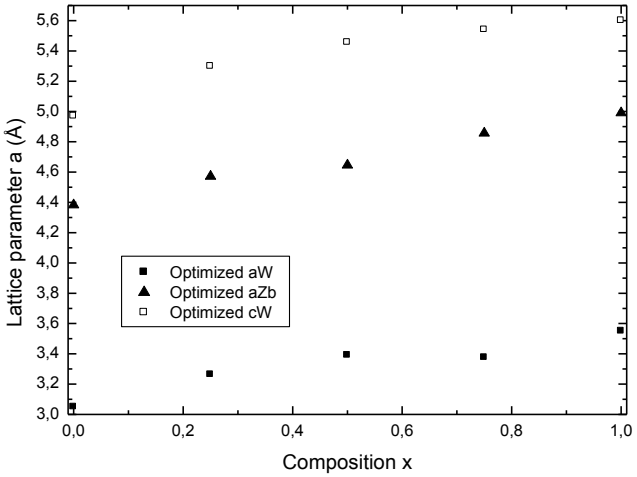

Fig. 1. Optimized lattice parameters of $Al_{1-x}In_xN$ in zincblende (a_{zb}) and wurtzite (a_w, c_w) phases.

The composition variation of lattice parameters for zincblende and wurtzite phases of $Al_{1-x}In_xN$ ternary alloy can be expressed in terms of the lattice parameters of AlN and InN binaries by using the virtual crystal approximation:

$$a(x) = xa_{AlN} + (1-x)a_{InN} + bx(1-x), \quad \textbf{(7)}$$

$$c(x) = xc_{AlN} + (1-x)c_{InN} + bx(1-x), \quad \textbf{(8)}$$

where b is the lattice bowing parameter.

Figure 1 shows a small deviation from linearity with a bowing parameter of b_{azb} = 0.0313 Å in the zincblende case, whereas for the wurtzite a slight deviation from linearity for parameter a(b_{awz}=-0.1326 Å) and a larger one for parameter c (b_{cwz} = -0.3726Å) are observed. The lattice mismatch between the two binaries is 13.87% in zincblende phase and 13.65% in wurtzite phase for parameter a and14.58% for parameter c.

3.2 Band structures

In zincblende phase AlN is shown to be indirect gap with DFT (TBM) calculated gap values at X and Γ points respectively 5.027 eV (4.92eV) and 5.60 eV (5.4 eV) compared to recommended values of 4.90 and 5.4 eV [14,15]. On the other hand, InN binary has a direct gap with a DFT (TBM) value of 0.86 eV(0.6374 eV) compared to experimental value of 0.61 eV [16]. In wurtzite phase, however both AlN and InN materials have a direct gap with DFT (TBM) calculated values 5.95 eV (6.231 eV) and 0.99 eV(0.79 eV) respectively compared to experimental values of 6.23 eV and 0.78eV [15].**Table 3** summarizes the calculations of $Al_{1-x}In_xN$ bandgap at Γ and X points at various compositions in zinc blende phase with comparison with other theoretical and experimental works. The gap remains direct except for In composition less than 0.25. In TBM (DFT) the crossover appears at x = 0.17 (0.10) with a gap of 4.47 eV (4.95). B-T. This is compared with other theoretical studies: Liou [17] found a crossover at x = 0.183 with a gap Eg = 4.972 eV and F.Wang [18] found at x = 0.18 for a gap Eg = 4.36 eV.

Table 3. Calculated and experimental band gap for AlN, InN and their alloys $Al_{1-x}In_xN$ in zincblende phase.

		AlN	$Al_{0.75}In_{0.25}N$	$Al_{0.50}In_{0.50}N$	$Al_{0.25}In_{0.75}N$	InN
NN sp3s TBM*	$Eg^{\Gamma-\Gamma}$ (eV)	5.4	4.043	2.774	1.624	0.6374
	$Eg^{\Gamma-X}$ (eV)	4.92	4.262	3.636	3.069	2.593
DFT-mBJLDA	$Eg^{\Gamma-\Gamma}$ (eV)	5.65216	3.68571	2.68908	1.57284	0.83204
	$Eg^{\Gamma-X}$ (eV)	5.08754	5.89543	4.53047	4.32746	4.18398
Others	$Eg^{\Gamma-\Gamma}$ (eV)	6.53[a], 5.4[b], 4.36[c], 4.25[d], 6.00[e]	4.70[f]		2.20[f]	0.53[a], 0.78[b], 0.0[d], 0.013[g], 0.73[h]
	$Eg^{\Gamma-X}$ (eV)	5.63[a], 4.9[b], 2.50[i], 3.23[j], 3.16[d], 4.90[e]				2.51[b], 1.56[d], 2.81[j]
Experiment		5.34[a]				0.7[i], 0.6[k], (0.7-1.1)[l]

a: Ref. [13], b: Ref. [15], c: Ref. [21], d: Ref. [40], e: Ref. [41], f: Ref. [39], g: Ref. [28], h: Ref. [23], i: Ref. [18], j: Ref. [21], k: Ref. [16], l: Ref. [37].

Figure 2 illustrates the band gap variation with the composition obtained by tight binding method (TBM) and density functional theory with modified Becke–Johnson potential (DFT-mBJLDA), in the two phases.

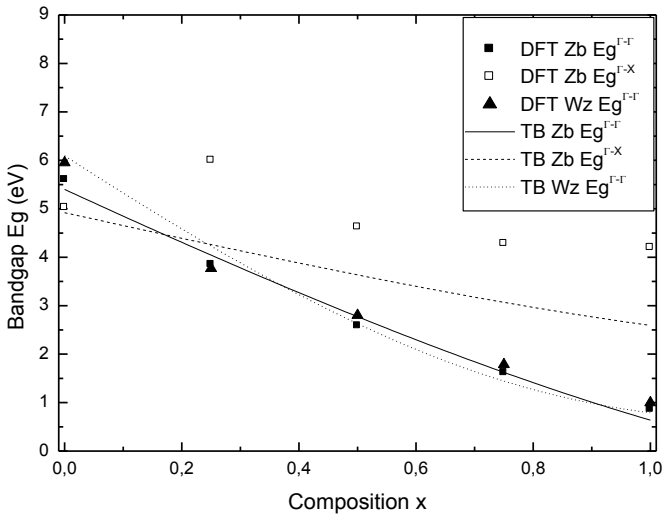

Fig. 2. *$Al_{1-x}In_xN$* zincblende and wurtzite band gap resulting from NN sp^3s^* TBM and DFT-mBJLDA calculations.

$Al_{1-x}In_xN$ band gaps in wurtzite phase are presented with both TBM and DFT-mBJLDA in **Table 4** along with other theoretical and experimental works. The results of the direct gap are approaching the experimental values better than other data with a higher accuracy in TBM. With the experimental values of the lattice parameter we obtained a gap in the direction gamma for binaries AlN (InN) 5.600 eV (0.861 eV) and in the X gap 5.027 eV (4.201 eV). For ternary with experimental values and using VCA to calculate lattice parameters (0.25, 0.50, 0.75) and we obtained for AlN (InN) theΓ (X) gap values [3.853 eV (6.004 eV), 2.5858 eV (4.627 eV) 1.616 eV (4.287 eV). These results are comparable with those obtained by optimization.

Table 4. Calculated and experimental band gap for AlN, InN and their alloys$Al_{1-x}In_xN$ in wurtzite phase

		AlN	$Al_{0.75}In_{0.25}N$	$Al_{0.50}In_{0.50}N$	$Al_{0.25}In_{0.75}N$	InN
NN sp3s TBM*	$Eg^{\Gamma-\Gamma}$ (eV)	6.231	4.303	2.656	1.448	0.7902
DFT-mBJLDA	$Eg^{\Gamma-\Gamma}$ (eV)	5.95008	3.76948	2.80204	1.78627	0.99784
Others	$Eg^{\Gamma-\Gamma}$ (eV)	4.85[a], 6.47[b], ((4.1671,5.0021),(3.9379, 4.7544))[c], 4.11[d], 4.027[e], (5.08, 4.24)[f], (4.50, 6.06)[g],	2.97[a]	1.47[a]	0.75[a]	0.0[a], 0.69[b], 0.90[h], ((0.000, 0.357), (0.000, 0.1716))[c], 0.299[e], (0.38, 0.26)[f],(-0.03, 0.95)[i],
Experiment		6.28[j], 6.23[k], 6.25[l]				0.9[b], (0.7-1.1)[g], 0.78[k], (0.7-0.9)[l], 0.7[m+n]

a: Ref. [32], b: Ref. [13], c: Ref. [34], d: Ref. [33], e: Ref. [35], f: Ref. [36], g: Ref. [37], h: Ref. [23], i: Ref. [42], j: Ref. [1], k: Ref. [15], l: Ref. [42], m: Ref. [18], n: Ref. [43].

Generally speaking, the band gap energy of *$Al_{1-x}In_xN$* can be approximately expressed as

$$E_g(x) = xE_{g\,AlN} + (1-x)E_{g\,InN} + bx(1-x), \quad (9)$$

where Eg (x) is the band gap energy of *$Al_{1-x}In_xN$* ternary alloy, $E_{gInN}$and E_{gAlN} are respectively, the band gap of InN and AlN binaries. b is the band gap bowing parameter for *$Al_{1-x}In_xN$* ternary. The obtained values of b are presented in **Table 5** showing a larger factor for wurtzite compared to zinc blende results probably attributed to a larger band gap in the wurtzite phase. They seem to be in good agreement with other calculations.

(9)

Table 5. Band gap bowing parameter of zincblende and wurtzite AlInN from tight binding and DFT (mBJLDA) calculations.

		NN sp3s TBM*	*DFT-mBJLDA*	*Others*
Zb-AlInN	$b^{\Gamma-\Gamma}$	0.9826	2.6648	2.5[a], (4.731 ± 0.794)[b], 3.851[c]
	$b^{\Gamma-X}$	0.4834	0.4262	(0.462 ± 0.285)[b], 0.104[c]
Wz-AlInN	$b^{\Gamma-\Gamma}$	3.4050	3.1269	3.4743[d], (2.7, 3.4x+1.2)[e]

a: Ref. [15], b: Ref. [17], c: Ref. [21], d: Ref. [32], e: Ref. [42].

In addition to band gap, another significant physical parameter in electronic transport for engineering electronic devices is the effective mass of free electrons and holes. The electronic mass calculation has been performed near the conduction band edge around Γ-point using a quadratic fit, the results of which are presented in **Tables 6 and 7** along with experimental and some other first principle calculations. The obtained data are in accordance with other calculations confirming a slight overestimation of DFT results, over experimental ones, inherent to the use of mBJLDA method [19]. These results also show similarities between the effective masses of the two phases and corroborate the lightness of the InN electron effective mass.

Table 6. Electron effective masses from *NN sp3s* TBM* and *DFT-mBJLDA* calculations for AlN, InN and their alloys in wurtzite phase with other works.

		AlN	$Al_{0.75}In_{0.25}N$	$Al_{0.50}In_{0.50}N$	$Al_{0.25}In_{0.75}N$	InN
NN sp3s TBM*	m_e/m_0	0.3096	0.2404	0.1712	0.1227	0.0948
DFT-mBJLDA	m_e/m_0	0.337	0.1851	0.1535	0.1233	0.1053
Others	m_e/m_0	0.2956[a]				0.1146[a]
Experiment	m_e/m_0	0.29 - 0.45[b]				0.07[b]

a: Ref. [35], b: Ref. [13]

Table 7 . Electron effective masses from tight binding and DFT calculations for AlN, InN and their alloys in zinc blende phase with other works.

		AlN	$Al_{0.75}In_{0.25}N$	$Al_{0.50}In_{0.50}N$	$Al_{0.25}In_{0.75}N$	InN
NN sp3s TBM*	m_e/m_0	0.318	0.2502	0.1846	0.1189	0.0519
DFT-mBJLDA	m_e/m_0	0.2903	0.1718	0.1430	0.1131	0.085
Others	m_e/m_0	0.32[a], 0.33[b], 0.25[c]				0.05[a], 0.07[c]
Experiment	m_e/m_0	---				0.04[d]

a: Ref. [1], b: Ref. [13], c: Ref. [15], d: Ref. [44]

Plots of electron effective mass versus composition for zincblende and wurtzite phases calculated by TBM and DFT-mBJLDA are illustrated in **Fig. 3** showing an almost linear variation with composition for both phases and a lighter mass for increasing x hence a higher carrier mobility more favorable in rich Indium $Al_{1-x}In_xN$ ternary.

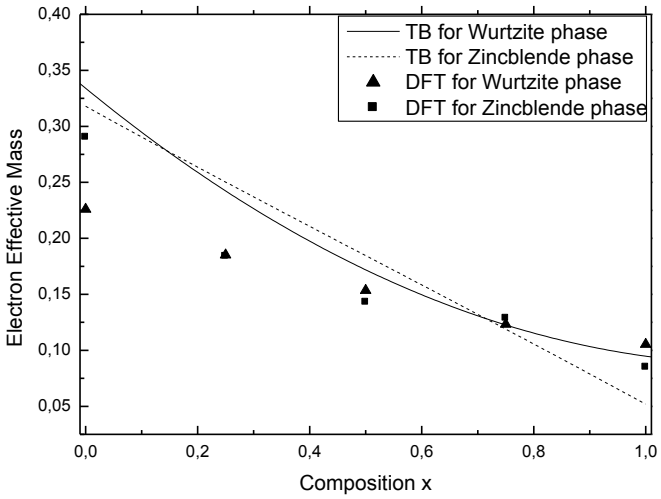

Fig. 3.$Al_{1-x}In_xN$ zincblende and wurtzite electron effective mass versus indium composition from NN sp^3s^*TBM and DFT-mBJLDA calculations.

3.3 Density of states and charge density:

The density of states, defined as the number of states allowed per energy unit, allows understanding the electronic properties. The calculated total and partial density of states are shown in **Figs. 4 and 5**, respectively, where the vertical dashed line represents the Fermi level which is set to zero. Clearly, the density of states is higher in wurtzite phase than in zincblende phase. The upper energy valence bands range from -5 eV to 0 eV. The major contribution comes from the nitrogen atom for all compositions in two phases. The p orbital seems to bring all the contribution of nitrogen to the binaries. The lower conduction band of wurtzite phase extends continuously from the value of the gap up to about 15 eV with a similar

contribution of all atoms either in wurtzite or zincblende phase. In the case of AlN the p orbital is prevalent while for InN the N contributes through the p and In through s orbitals. The ternary compounds present in the case of wurtzite a continuous lower conduction band whereas for zincblende there is a discontinuity that seems to shift towards higher energies with augmenting indium content. In the case of the valence band we notice that the DOS peak increases with indium.

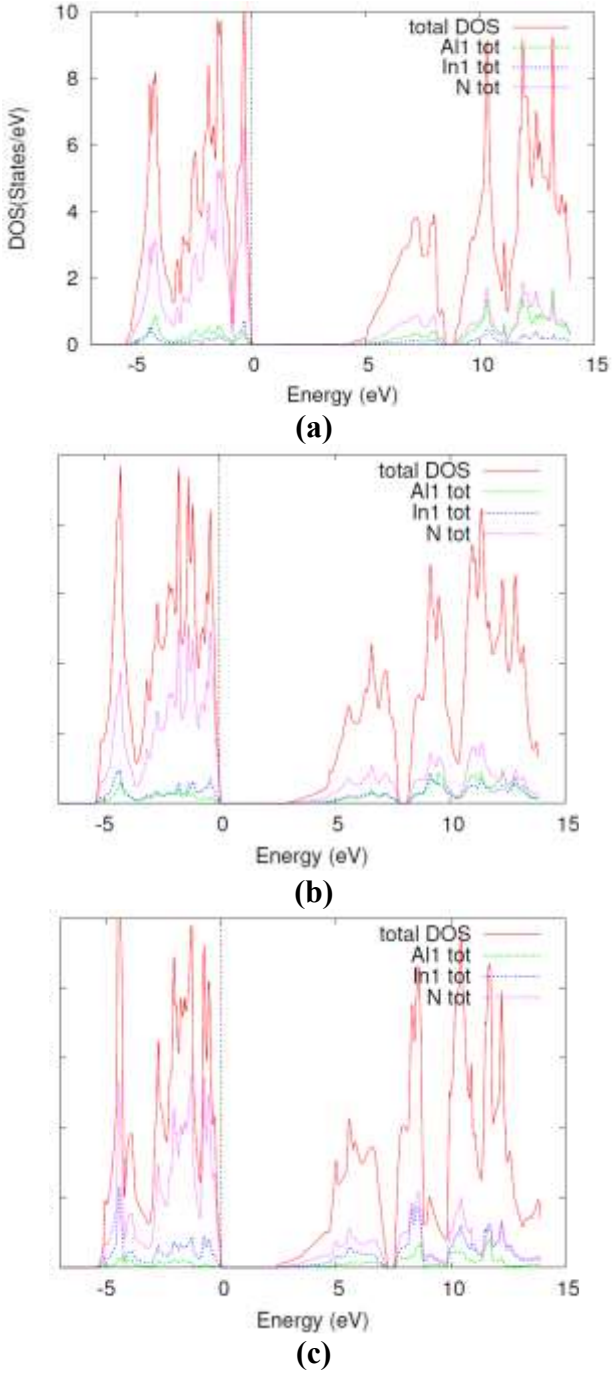

Fig. 4 Total and partial density of states of zincblende $Al_{1-x}In_xN$: x=0.25 (a), 0.50 (b) and 0.75 (c).

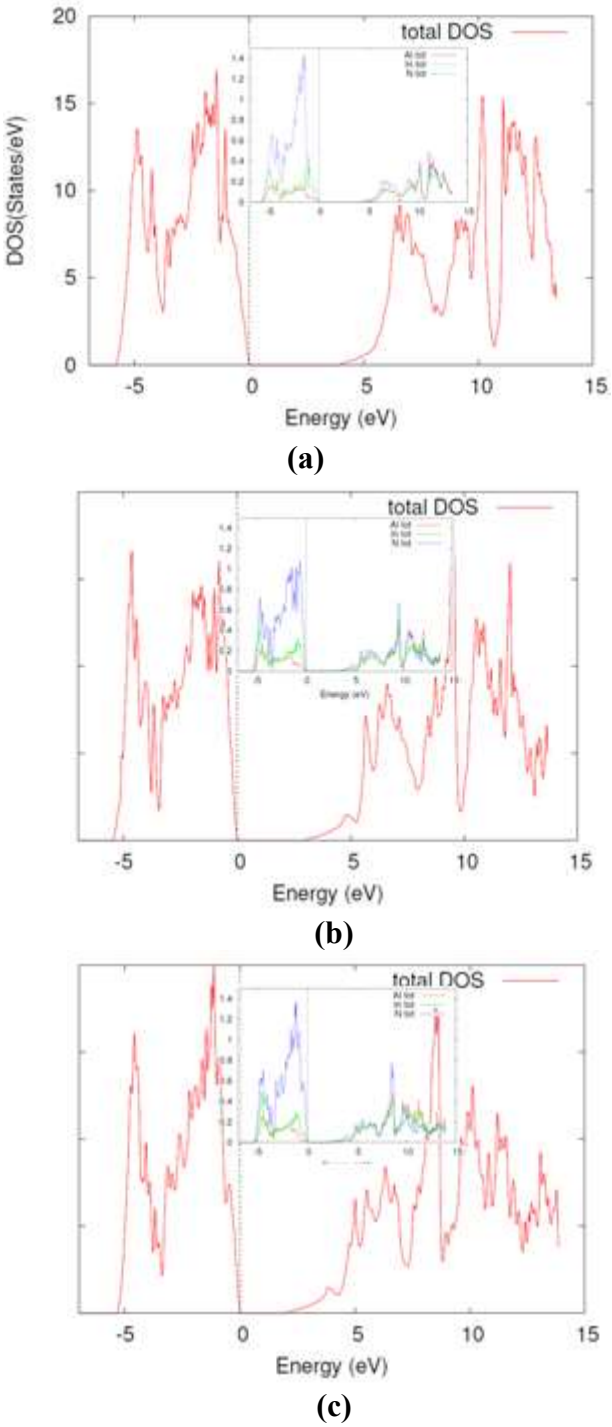

Fig. 5 Total and partial density of states of wurtzite $Al_{1-x}In_xN$:x=0.25 (a), 0.50 (b) and 0.75 (c).

The emphasis here is to seek why the inclusion of Indium ion tend to a crossover of the band gap. It is useful to point out that, in wurtzite, the lattice periodicity along certain direction is expanded to several times than in the case of zinc blende structure. Besides, the structures have lattice distortions, e.g., non-ideal *c/a* ratio, and internal interatomic distance relaxations. These geometrical changes cause thus, the splitting of the top of the valence band and introduce couplings between the Brillouin zone folded states, which are the origin of the large reduction of

the band gaps value. The key idea to give an accuracy analysis of this trend is to explore the chemical bonding behavior. Thanks to the opportunity that offered by the quantum chemical topology formalism [45-47], the use of the electron localization index (ELF) may help to pinpoint the nature of chemical bonds of the studied alloys. The substitution of a cation like the aluminum shown negligible inwards movements towards the nitrogen atom. This result indicates a no significant coupling between the off-center Al and its host.

The inclusion of the aluminum atom affects weakly the nature of the super cell. It is shown from **Figs.6 and 7**, a formation of the Al—N polarizable bonds with electron localization index equal to 0.88. And, a monosynaptic basin with an order of a valence ELF=0.86/0.85 (lone pair) located along the In—N bond. The differences observed in the ELF basins are directly related with the atomic environment of each atom. The tendency is common: the presence of Al or In cations does not affect the hardly the properties of the alloy, bonding behavior in all bond is ionic. However, it is interesting to said that, while incorporating the Al cation, we show that the bond being as a perturbed lone pair one, this is due essentially to the change of the electronegativity of the substituted atom, in fact now we have a single bond plus a lone pair one. Also, it worth noting that, the Al—N seems to be slightly strongest than In—N one, since its polarizable character.

The listed properties in **Table 8** confirm this trend. The total magnitude of first dipole arises while the Al concentration is increased in the wurtzite alloy. However, the population of valence-electron emerges with adding the In ions. In fact, ELF analysis of the bonds show that the most valence charge is mainly formed by the Indium one, while the most Al one become rather polarizable (Al^{+3}—N^{-3}). The polarization contribution between atoms is mainly affected by the charge transfer between Al—N ions. Where, the valence basin center is located at this attractor position forming the bonds. In the case of bonds, attractors do not systematically localized on the bond midpoint and their localization depends on electronegativity differences between the atoms forming the bond and on the nature of the chemical environment. Furthermore, the included cation causes a polarizable bond and more the electron wave function of the electron become extended, due of the increase of the flatness index with Al substitution. In a polar semiconductor with ionic bond (Laplacian $\nabla^2\rho > 0$) like the $Al_{1-x}In_xN$, there is no unique way of assigning charge to each atom, but there are some logical ways to proceed. In fact, the electron charge distribution along the bond becomes asymmetric, with a tendency for electrons to transfer from the d/p-Al orbitals to the lower-energy anion (s-N orbitals).

Table 8. Integrated properties from ELF analysis of the alloys$Al_{1-x}In_xN$ in wurtzite phase.

Alloy	Flatness(%)	Electronic bonding population (electron/bohr)	$\nabla^2\rho$ of In—N/Al—N Bonds(electron/bohr)	*Magnitude of first dipole moment* (electrons.bohr)
$Al_{0.75}In_{0.25}N$	8.51	360.962	0.44/0.27	122.07
$Al_{0.50}In_{0.50}N$	8.61	400.482	0.34/0.22	114.85
$Al_{0.25}In_{0.75}N$	8.92	446.669	0.29/0.17	137.79

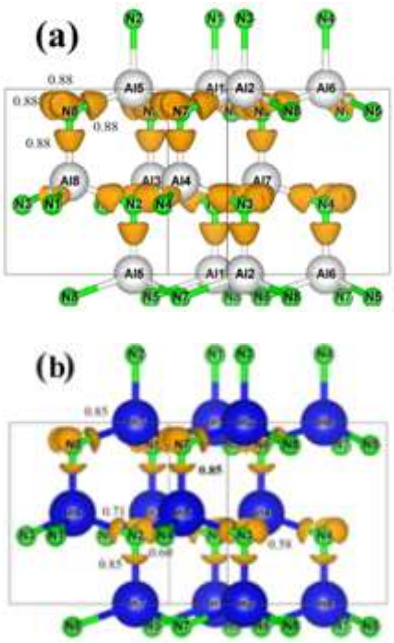

Fig. 6 ELF isosurface of AlN and InN in wurtzite phase along the x concentration x=0 (a), 1(b).

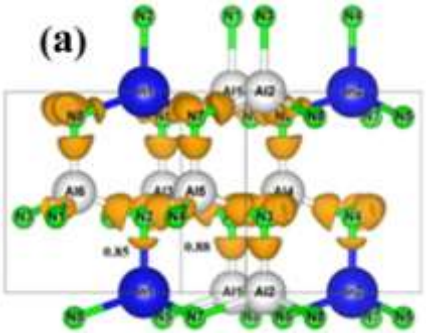

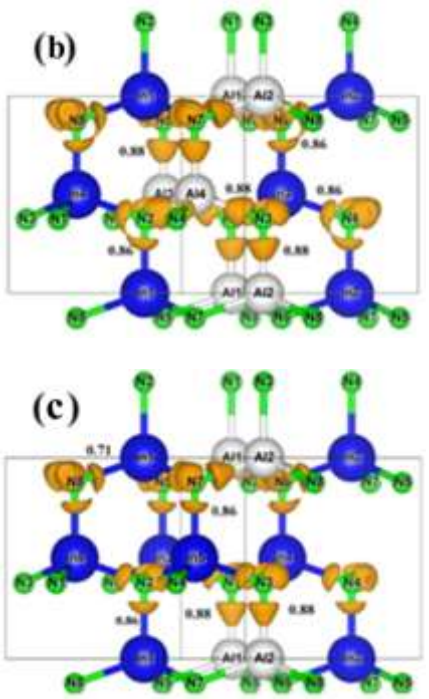

Fig. 7 ELF isosurface of $Al_{1-x}In_xN$ in wurtzite phase along the x concentration x=0.25 (a), 0.50 (b), 0.75 (c).

4. CONCLUSION

We presented a comparative theoretical study on structural and electronic properties of AlN and InN binaries and their ternary alloy $Al_{1-x}In_xN$ by using NN sp^3s^* TBM and DFT-mBJLDA. The structural part of the study showed a good agreement between calculated values and experimental works. Concerning the electronic properties using the DFT-mBJLDA yielded better gap results than other DFT works while using the NNsp^3s^* TBM gives satisfactory results for the gap and effective mass and more accurate gaps than DFT-mBJLDA.

While for effective masses there seems no noticeable differences between the zincblende and wurtzite phases, the results of the gap on the other hand are quite different: From being direct throughout the entire range and with values ranging from 6.2 to 0.79 eV for the wurtzite to being indirect at first then direct and with a smaller span ranging from 5.4 to 0.63 eV for the zincblende. Concerning the DOS a higher total density for the wurtzite phase is being observed in the work. Partial contributions from different orbitals have also been reported.

Acknowledgement

The authors are grateful to the Algerian ministry of higher education and scientific research for their financial support.

References

[1] J. Wu, "When group-III nitrides go infrared: New properties and perspectives" J. Appl. Phys. vol. 106 N°1, 011101 (2009).

[2] J. Kuzmik. Power electronics on InAlN/(In)GaN: Prospect for a record performance. IEEE
Electron Device Lett., 22:510, 2001.

[3] R Butté, J. F. Carlin, E. Feltin, M. Gonschorek, S. Nicolay, G. Christmann, D. Simeonov, A. Castiglia, G. Dorsaz and H. J. Buehlmann, "Current status of AlInN layers lattice-matched to GaN for photonics and electronics", J. Phys. D: Appl. Phys. Vol.40, pp. 6328–6344, (2007)

[4]D. J. As, D. Schikora, and K. Lischka, "Molecular beam epitaxy of cubic III-nitrides on GaAs substrates", Phys. stat. sol. (c), vol. 0, No. 6, pp. 1607–1626, (2003)

[5] F. Tran, P. Blaha, "Accurate band gaps of semiconductors and insulators with a semilocal exchange-correlation potential", Physical Review Letters 102 226401, (2009).

[6] P. Blaha, K. Schwarz, G.H. Madsen, D. Kvasnicka, J. Luitz, FP-L/APW +lo Program for Calculating Crystal Properties, Vienna University of Technology, Vienna, 2001.

[7] J. Perdew, K. Burke, M. Ernzerhof, "Generalized Gradient Approximation Made Simple", Phys. Rev. Lett. 77 (1996) 3865.

[8] H. Ünlü, H. H. Gürel, Ö. Akinci, and M. R. Karim, "Modeling of low dimensional Semiconductors: Characterisation, Modeling and Applications", (Eds) H. Ünlü, N. J. M. Horing, Springer 2013.

[9] O. Madelung, "Semiconductors group IV elements and III-V compounds", Springer-VerlagBelin Heidelberg, 1991.

[10] A. D. Becke, K. E. Edgecombe, "A simple measure of electron localization in atomic and molecular systems", J. Chem. Phys., 92 1990 1758.5397.

[11] M. Kohout, A. Savin, , "Atomic shell structure and electron numbers", Int. J. Quantum Chem. 1996, 60, pp. 875-882

[12] F.D. Murnaghan, Proc. Natl. Acad. Sci. USA 30 (1944) 244–247.

[13] P. Rinke, M. Winkelnkemper, A. Qteish, D. Bimberg, J. Neugebauer and M. Scheffler, "Consistent set of band parameters for the group-III nitrides AlN, GaN and InN", Phys. Rev. B 77, 075202 .(2008)

[14]Wang, S. Q. and Ye, H. Q.,2002,"A plane-wave pseudopotential study on III–V zinc-blende and wurtzite semiconductors under pressure", J. Phys.: Condens. Matter Vol.14, pp 9579- 9587.

[15] I. Vurgaftman and J.R. Meyer, "Band parameters for nitrogen-containing semiconductors", J. Appl. Phys. vol.36, N°6, pp. 3675-3696, (2003).

[16] J. Schörmann, D. J. As, K. Lischka, P. Schley, R. Goldhahn, S.F. Li, W. Löffler,. Hetterich and H. Kalt, "Molecular beam epitaxy of phase pure cubic InN", Appl. Phys. Lett. 89,261903 (2006).

[17] B.-T. Liou and C.-W.Liu, "Electronic and structural properties of zinc blende $Al_xIn_{1-x}N$", Optics Communications 274, pp. 361-365, (2007).
[18] Fei Wang, S.F. Li, Qiang Sun, Yu Jia, "First-principles study of structural and electronic properties of zincblende $Al_xIn_{1-x}N$",Solid State Sciences 12, pp. 1641-1644, (2010).
[19] R. B. Araujo, J. S. de Almeida, A. Ferreira de Silva, "Electronic properties of III nitride semiconductors: A first-principles investigation using the Tran-Blaha modified Becke-Johnson potential" J. Appl. Phys 114, 183702 (2013).
[20] Zhao-Yong Jiao, Shu-Hong Ma and Ji-Fei Yang,"A comparison of the electronic and optical properties of zinc-blende, rocksalt and wurtzite AlN: A DFT stufy", Solid State Sciences 13, pp. 331-336, (2011).
[21] M. B. Kanoun, S. Goumri-Said, A. E. Merad, and H. Mariette, "Ab initio study of structural parameters and gap bowing in zinc-blende $Al_xGa_{1-x}N$ and $Al_xIn_{1-x}N$ alloys" J. Appl. Phys. 98, 063710 (2005).
[22] C. Pearson, A. Ferreira da Silva, A. Ahuja and B. Johansson, "Effective electronic masses in wurtzite and zinc-blende GaN and AlN, J. Cryst. Growth 231,pp. 397-406, (2001).
[23] Bakhtiar UlHaq, R. Ahmed, A. Shaari, F. ElHaj Hassan, Mohammed Benali Kanoun and Souraya Goumri-Said, "Study of wurtzite and zincblende GaN/InN based solar cells alloys: First-principles investigation within the improved modified Becke-Johnson potential", solar Energy 107,pp. 543-552, (2014).
[24] Mohamed Issam Ziane, Zouaoui Bensaad, Tarik Ouahrani and Hamza Bennacer, " First principles study of structural, electronic and optical properties of indium gallium nitride arsenide lattice matched to gallium arsenide", Materials Science in Semconductor Processing 30,pp. 181-196, (2015).
[25] M. J. Winiarski, M. Polak and P. Scharoch, "Anomalous band-gap bowing of $AlN_{1-x}P_x$ alloy, Journal of Alloys and Compounds, Vol. 575, pp 158-161, (2013).
[26] A. Laref, A. Altujar and S. J. Luo, " The electronic and optical properties of InGaN-based solar cells alloys: First-principles investigations via mBJLDA approach", Eur. Phys. J. B (2013)86: 475.
[27] S. Goumri-Said, M. B. Kanoun, A. E. Merad, G. Merad and H. Aourag, Chem. Phys. 302, p. 135, (2004).
[28] I. Petrov, K. Mojab, R. C. Powell, J. E. Greene, Appl. Phys. Lett. 60, 2491, (1992).
[29] R. Ahmed S. J. Hashemifar, H. Akbarzadeh, M. Ahmed and F. e-Aleem, Computational Materials Science 39, pp. 580-586, (2007).
[30] V. Cimalla, J. Pezoldt, G. Ecke, R. Kosiba, O. Ambacher, L. Spieβ, G. Teichert, H. Lu, W. J. Schaff, Appl. Phys. Lett. 83, 3468, (2003).
[31] Q. Yan, P. Rinke, M. Scheffler andC. G. Van de Walle, "Strain effects in group-III nitrides: Deformation potentials for AlN, GaN and InN", Apll. Phys. Lett.95, 121111 (2009).
[32] Q. Y. Chen, M. Xu, H. P. Zhou, M. Y. Duan, W. J. Zhu and H. L. He, "First-principles calculation of electronic structures and optical properties of wurtzite $In_xGa_{1-x}N$ alloys", Physica B 403, pp. 1666-1672, (2008).
[33] L. Shi, Y. Duan, X. Yang, G. Tang, L. Qin and L. Qiu, "Structural, electronic and elastic properties of wurtzite-structured $Ti_xAl_{1-x}N$ alloys from first principles", Materials Science in Semconductor Processing 15, pp. 499-504, (2012).
[34] R. Nunez-Gonzalez, A. Reyes-Serrato,A. Posada-Amarillas and D. H. Galvan, "First-principles calculation of the band gap of $Al_xGa_{1-x}N$ and $In_xGa_{1-x}N$", Revista Mexicana De Fisica S54 (2), pp. 111-118, (2008).
[35] E. Lopez-Apreza, J. Arriaga and D. Olguin"Ab initio calculation of structural and electronic properties of $Al_xGa_{1-x}N$ and $In_xGa_{1-x}N$ alloys", Revista Mexicana De Fisica 56 (3), pp. 183-194, (2010).
[36] S. Kumar, S. Pandey, S.K. Gupta, T. K. Maurya, P. Schley, G. Gobsch and R. Goldhahn; "Band structure and optical properties of hexagonal In-rich $In_xAl_{1-x}N$ alloys", J. Phys. Condens. Matter 23, 475801 (10pp) , (2011).
[37] S. Adachi, "Properties of Group-IV, III-V and II-VI Semiconductors", Wiley Series in Materials for Electronic & Optoelectronic Applications, (2005).
[38] S. Zhang, J.-j. Shi, S-g. Zhu, F. Wang, M. Yang and Z.-q. Bao, "Indium distribution and light emission in wurtzite InGaN alloys: Several-atom In-N clusters", Phys. Lett. A 374, pp. 4767-4773, (2010).
[39] M. Ferhat, F. Bechstedt, "First principles calculations of gap bowing in $In_xGa_{1-x}N$ and $Al_xIn_{1-x}N$ alloys: Relation to structural and thermodynamic properties", Phys. Rev. B65, 075213,(2002).
[40] S. Berrah, A. Boukortt and H. Abid, "The composition effect on the bowing parameter in the cubic InGaN, AlGaN and AlInN alloys", Semiconductor Physics, Quantum Electronics &Optoelectronics, V. 11, N1, pp. 59-62, (2008).
[41]M. Ferhat, A. Zaoui, M. Certier and B. Khelifa, "Empirical tight-binding band structure of zinc-blende nitrides GaN, AlN and BN", Phys. stat. sol. (b) 195, 415, (1996).
[42]R. R. Pelà, C. Caetano, M. Marques, L. G. Ferreira, J. Furthmüller and L. K. Teles, "Accurate band gaps of AlGaN, InGaN and AlInN alloys calculations based on LDA-1/2 approach", Appl. Phys. Lett., 98, 151907, (2011).
[43]F. Litimein, B. Bouhafs, G. Nouet and P. Ruterana, Phys. Status Solidi B 243, 1577 (2006).
[44] P. Schley, C. Naprerala, R. Goldhahn, G. Gobsch, J. Schörmann, D. J. As, K. Liscka, M. Feneberg, K. Thonke, F. Fuchs and F. Bechstedt, Phys. Status Solidi C 5, 2342 (2008).
[45] R. F. W. Bader, "Atoms in Molecules: A Quantum Theory", Oxford University Press, Oxford, 1990.
[46] R. F. W. Bader, P.M. Beddall, P.E. Cade, "Partitioning and characterization of molecular charge distributions", J. Am. Chem. Soc. 93 (13) (1971), pp. 3095-3107.
[47] K. E. Laidig, R. F. W. Bader, " Properties of atoms in molecules: Atomic polarizabilities", J. Chem. Phys. 93 (1990) 7213.